Journal of Traditional and Complementary Medicine 12 (2022) 260–268

Contents lists available at ScienceDirect

Journal of Traditional and Complementary Medicine

journal homepage: http://www.elsevier.com/locate/jtcme

In vitro effects and mechanisms of action of *Bidens pilosa* in *Trypanosoma brucei*

Aboagye Kwarteng Dofuor [a, c], Georgina Isabella Djameh [d], Michael Amoa-Bosompem [d], Samuel Kwain [e], Enoch Osei [e], Gilbert Mawuli Tetevi [e], Frederick Ayertey [f], Peter Bolah [f], Laud Kenneth Okine [a, b], Kwaku Kyeremeh [e], Theresa Manful Gwira [a, b, *], Mitsuko Ohashi [d, g, 1]

[a] *West African Centre for Cell Biology of Infectious Pathogens, University of Ghana, Legon, Ghana*
[b] *Department of Biochemistry, Cell and Molecular Biology, University of Ghana, Legon, Ghana*
[c] *Department of Biological, Physical and Mathematical Sciences, University of Environment and Sustainable Development, Somanya, Ghana*
[d] *Department of Parasitology, Noguchi Memorial Institute for Medical Research, University of Ghana, Legon, Ghana*
[e] *Marine and Plant Research Laboratory of Ghana, Department of Chemistry, University of Ghana, Legon, Ghana*
[f] *Center for Plant Medicine Research, Mampong-Akuapem, Ghana*
[g] *Department of Environmental Parasitology, Tokyo Medical and Dental University, Tokyo, Japan*

ARTICLE INFO

Article history:
Received 18 June 2020
Received in revised form
7 August 2021
Accepted 10 August 2021
Available online 11 August 2021

Keywords:
Asteraceae
Cell cycle
Apoptosis
Necrosis
Trypanosomatidae
African trypanosomiasis
Tryptophan esters

ABSTRACT

Background and aim: African trypanosomiasis poses serious health and economic concerns to humans and livestock in several sub-Saharan African countries. The aim of the present study was to identify the antitrypanosomal compounds from *B. pilosa* (whole plant) through a bioactivity-guided isolation and investigate the *in vitro* effects and mechanisms of action against *Trypanosoma brucei* (*T. brucei*).
Experimental procedure: Crude extracts and fractions were prepared from air-dried pulverized plant material of *B. pilosa* using the modified Kupchan method of solvent partitioning. The antitrypanosomal activities of the fractions were determined through cell viability analysis. Effects of fractions on cell death and cell cycle of *T. brucei* were determined using flow cytometry, while fluorescence microscopy was used to investigate alterations in cell morphology and distribution.
Results and conclusion: The solvent partitioning dichloromethane (BPFD) and methanol (BPFM) fractions of *B. pilosa* exhibited significant activities against *T. brucei* with respective half-maximal inhibitory concentrations (IC_{50}s) of 3.29 μg/ml and 5.86 μg/ml and resulted in the formation of clumpy subpopulation of *T. brucei* cells. Butyl (compound **1**) and propyl (compound **2**) esters of tryptophan were identified as the major antitrypanosomal compounds of *B. pilosa*. Compounds **1** and **2** exhibited significant antitrypanosomal effects with respective IC_{50} values of 0.66 and 1.46 μg/ml. At the IC_{50} values, both compounds significantly inhibited the cell cycle of *T. brucei* at the G0-G1 phase while causing an increase in G2-M phase. The results suggest that tryptophan esters may possess useful chemotherapeutic properties for the control of African trypanosomiasis.

Abbreviations: B. pilosa, *Bidens pilosa* L (whole plant); AT, African trypanosomiasis; HAT, Human African trypanosomiasis; AAT, Animal African trypanosomiasis; BPC, crude extract of *B. pilosa*; BPFD, Dichloromethane fraction of *B. pilosa*; BPFM, methanol fraction *B. pilosa*; BPWB, water-butanol fraction of *B. pilosa*; BPFH, hexane fraction of *B. pilosa*.

* Corresponding author. West African Center for Cell Biology of Infectious Pathogens, Department of Biochemistry, Cell and Molecular Biology, University of Ghana, P. O. Box LG54, Legon, Ghana.
E-mail address: tmanful@ug.edu.gh (T.M. Gwira).

Peer review under responsibility of The Center for Food and Biomolecules, National Taiwan University.

[1] Mitsuko Ohashi: Department of Parasitology, Noguchi Memorial Institute for Medical Research, University of Ghana, P.O. Box LG 581 Legon, Ghana; Department of Environmental Parasitology, Tokyo Medical and Dental University, Tokyo, Japan. **Current contact** - E-mail: mitsukoohashi0605@gmail.com.

https://doi.org/10.1016/j.jtcme.2021.08.008

1. Introduction

African trypanosomiasis (AT) is a tsetse-transmitted disease of humans (Human African trypanosomiasis, HAT) and animals (Animal African trypanosomiasis, AAT), caused by parasitic protozoans of the genus and family *Trypanosoma* and *Trypanosomatidae* respectively. HAT afflicts an estimated 70 million population in several sub-Saharan African countries.[1] In addition, AAT affects millions of people living in sub-Saharan Africa as this animal disease impairs livestock breeding and can lead to considerable losses in productivity of livestock and economy. Moreover, AAT, which continues to threaten the lives of several million herds of cattle every year, needs new approaches to combat the disease.[2]

Vaccine development for AT is beset with various challenges, part of which is due to the several immune evasion strategies adopted by the parasite.[3] Chemotherapy, which is the most economically viable option,[4,5] faces challenges of drug resistance, adverse side effects, and difficulty in regimen application.[6–9] Coupled with the fact that more than half of the world population depends on traditional medicinal products,[10] natural products from plants may provide an alternative source of viable chemotherapy.

Bidens is a genus of mostly annual or perennial herbaceous plants that belongs to the family of *Asteraceae* with at least 200 species.[11] *Bidens pilosa* L. (*B. pilosa*), probably the most studied species of the genus, is a glaborous or hairy plant traditionally considered to be of an important medicinal, nutritional and ethnomedical relevance.[12] Even though South America may be considered as the original source, the species may be found in different parts of Africa, America, Polynesia, Europe and Asia.[13] Due to its invasive, fast-growing and prolific nature, the species may also be considered a weed.[14] Moreover, several pharmacological properties such as antidiabetic, anticancer, anti-inflammatory, antioxidant, immunomodulatory, antibacterial and antimalarial activities have been reported on extracts and isolated agents of *B. pilosa*.[12] Many secondary metabolites including aliphatics, flavonoids, phenyl propanoids, aromatics and porphyrins that have been isolated from *B. pilosa* may thus be largely responsible for its diverse pharmacological properties.[12,15]

Extracts of *B. pilosa* were reported to exhibit *in vitro* and *in vivo* activities against *Trypanosoma brucei* (*T. brucei*).[16,17] However, the mechanisms of antitrypanosomal action of the plant was not investigated. Insights into the effects and mechanisms of action of *B. pilosa* may promote the development of novel antitrypanosomal drugs through which challenges associated with currently available antitrypanosomal drugs could be overcome**.** The aim of the present study was thus to identify the active fractions of the Ghanaian species of *B. pilosa* (whole plant), as well as to determine their effects and mechanisms of action using a panel of selected cell biological methods.

2. Materials and methods

2.1. Culture of parasites and human cell lines

Blood stream forms of *T. brucei* (GUTat 3.1 strains) and Jurkat cells were cultured *in vitro* to the logarithm phase using Hirumi's Modified Iscove's Medium (HMI9, Thermo Fisher Scientific) with 10% foetal bovine serum (Thermo Fisher Scientific) at 5% CO_2 and 37 °C. Chang liver (HeLa derivative) cell lines were cultured *in vitro* to the logarithm phase using Minimum Essential Medium (MEM, Thermo Fisher Scientific) with 10% foetal bovine serum at 5% CO_2 and 37 °C. Macrophages (RAW 264.7 cell lines) were cultivated *in vitro* to the logarithm phase using Dulbecco's Modified Eagle Media (DMEM, Thermo Fisher Scientific) with 10% foetal bovine serum at 5% CO_2 and 37 °C.

2.2. Crude extraction and fractionation of plants

The whole plant of *B. pilosa* was collected from the arboretum of the Center for Plant Medicine Research (CPMR), Mampong-Akuapem, Ghana. The plant was authenticated and given the voucher specimen number CPMR 4123/4124/4125. Crude extracts and fractions were prepared from the air-dried pulverized plant material using a modified version of the Kupchan method of solvent extraction,[18] as illustrated schematically in Supplementary Fig. S1. Briefly, the pulverized air-dried plant material was soaked in absolute dichloromethane and left to percolate at room temperature for 1 week. The dichloromethane extracts were decanted and filtered through a mixture of cotton and glass wool. The plant material was then soaked in absolute methanol for another week after which the methanol extract was also decanted and filtered. The methanol and dichloromethane extracts were combined and dried under vacuum with a Heidolph Rotavap (40 °C, 1 atm) to give the total crude extract (TCE). The TCE was suspended in water and extracted three times with absolute dichloromethane. The remaining aqueous layer was then extracted once with absolute *sec*-butanol and the butanol fraction was dried under vacuum to produce the water-butanol (WB) fraction. The dichloromethane layer was dried under vacuum and the extract was suspended in a 1:9 mixture of water and methanol. This fraction was then extracted three times with absolute hexane after which the hexane layer was dried under vacuum to give the hexane (FH) fraction. The remaining 1:9 mixture of water and methanol layer was phase adjusted to a 1:1 mixture, extracted three times with dichloromethane and dried under vacuum to give the dichloromethane (FD) fraction. The 1:1 water-methanol layer was also dried under vacuum to give the FM fraction.

2.3. Chromatographic and spectrometric analysis

Analytical normal phase silica-coated thin layer chromatography (TLC) was repeatedly run on both Kupchan and gravity column fractions to estimate the levels of polarity and purity of all fractions, as well as to determine the appropriate solvent systems for silica gel gravity column chromatography. The solvent systems used in TLCs were selected based on the specific Kupchan fractions (FH, FD, FM, and WB) under investigation. For the FD and FM fractions, the solvents used were ethylacetate, dichloromethane, hexane and occasionally methanol to facilitate the movement of highly polar compounds on normal phase. The data obtained from TLC runs were used to set up gravity column chromatography. Apart from observing TLC plates under both long (365 nm) and short (254 nm) UV wavelengths, phytochemical screening of TLC spots was conducted using a number of reagents such as iodine, ninhydrin, Dragendorff and antimony (III) chloride. For the ninhydrin and antimony (III) chloride tests, TLC spots were developed in 10% H_2SO_4 with heating at 110 °C. Appropriate solvent systems for silica gel gravity column chromatography were selected following successful TLC runs. Silica gel gravity column chromatography was used for further purification of plant extracts following Kupchan solvent partitioning. The column used for this chromatographic step was 120 cm long and 2.5 cm wide with ethyl acetate, hexane and methanol routinely used as mobile phases. Briefly, the methanol fraction (FM) obtained from Kupchan solvent partitioning was loaded on a glass column containing silica gel packed to the 80 cm mark. The column was subjected to gradient elution using a mixture of *n*-hexane and ethyl acetate (90/10, 80/20, 70/30, 60/40, 50/50, 40/60, 30/70, 20/80, and 0/100). The remaining compounds on the silica column were then flushed out using 100% methanol.

Semi-preparative HPLC purifications were carried out using a Phenomenex Luna reverse-phase (C18 250 × 10 mm, L × i.d.)

column connected to a Waters 1525 Binary HPLC pump chromatograph with a 2998 photodiode array detector (PDA), column heater, and in-line degasser. Detection was achieved on-line through a scan of wavelengths from 200 to 400 nm, using a solvent system of A = 80/20 (H_2O/CH_3CN) and B = 95/5 (CH_3CN/H_2O) in 30 min and held in 100% CH_3CN for 20 min. About 3.5 and 3.2 mg, respectively, of compounds **1** and **2** were obtained after 48 h injections.

Gas chromatography-mass spectrometric (GC-MS) analysis was performed using a PerkinElmer GC Clarus 580 Gas Chromatograph interfaced to a Mass Spectrometer PerkinElmer (Clarus SQ 8S) equipped with Elite-5MS (5% diphenyl/95% dimethyl polysiloxane) fused to a capillary column (L × I.D. 30 m × 0.25 mm, df 0.25 μm). The oven temperature was programmed from 40 °C with an increase of 3 °C/min to 90 °C, then 10 °C/min to 240 °C and holding for 15 min at 240 °C. For GC-MS detection, an electron ionization system was operated in electron impact mode with ionization energy of 70 eV. Helium gas (99.999%) was used as a carrier gas at a constant flow rate of 1 ml/min and an injection volume of 1 μL. The injector temperature was maintained at 250 °C with an ion-source temperature of 150 °C. Mass spectrum was taken at 70 eV with a scan interval of 0.1 s and fragments from 45 to 450 Da. The solvent delay was 0–2 min. The total GC-MS running time was approximately 40 min. The mass-detector used in this analysis was a PerkinElmer TurboMass and the software adopted was a TurboMass version 6.1.0. Interpretation of mass spectra was carried out using the database of National Institute of Standard and Technology (NIST) with at least 62,000 patterns.

2.4. Analysis of cell viability and cytotoxicity

Determination of cell viability was based on a colorimetric analysis involving resazurin19. For *T. b. brucei* and Jurkat, cells were seeded at a density of 3.0×10^5 cells/ml on 96-well plates in a two-fold dilution of fractions or compounds. RAW 264.7 and Chang liver (HeLa derivative) cell lines were plated at a density of 3.0×10^5 cells/ml for 48 h to allow for sufficient adherence to plates. For all cell types, fractions or compounds were incubated in a two-fold dilution with resazurin (10% V/V) for another 24 h to allow for a complete color development. All experiments were run in triplicates. Spectrophotometric absorbance was recorded at a wavelength of 570 nm. Diminazine aceturate (DA), a commercially available antitrypanosomal drug, was used as a positive control.

2.5. Analysis of apoptosis and necrosis

Flow cytometry-based detection of apoptosis- and necrosis-like cell death using annexin-V and 7-amino actinomycin-D was employed.[20] We followed the same procedures and protocols as previously described.[21] Parasites were seeded at a density of 3.0×10^5 cells/ml with or without fractions/compounds. Nexin reagent containing annexin-V and 7-amino actinomycin-D was used for the identification of apoptosis-like and necrosis-like cell death as previously demonstrated.[21] Data was generated as dot plots with the guava easycyte HT flow cytometer. Five thousand cells per sample were counted in each experiment.

2.6. Analysis of cell cycle

The cell cycle assay was based on a univariate analysis of DNA content upon staining with propidium iodide.[22] We followed the same procedures as previously described.[21] Parasites were seeded at a density of 3.0×10^5 cells/ml with or without fractions/compounds. Cells were washed in PBS and fixed in ethanol. Guava cell cycle reagent containing propidium iodide was used for the detection and quantification of DNA as shown in our previous study.[21] Distribution of cells at distinct cell cycle phases was measured with the BD LSFortessa X-20 flow cytometer. Five thousand cells per sample were counted in each experiment.

2.7. Fluorescence microscopy

We followed the same procedures as established in our previous report.[21] Parasites were seeded at a density of 3.0×10^5 cells/ml with or without fractions/compounds. Cells were fixed in paraformaldehyde, washed appropriately and alternately in PBS and PBST, before finally incubated in 4', 6-diamidino-2-phenylindole (DAPI) as described previously.[21] Data was analysed with the CellSens standard imaging software and Adobe Photoshop CS6.

2.8. Statistical analysis

Data from cell viability assay was analysed with Graphpad Prism version 5. The half-maximal inhibitory concentration (IC_{50}) was calculated as the concentration that caused a 50% reduction in cell viability. IC_{50} values were calculated from a non-linear regression model. Dot plots from cell death and cell cycle assays were analysed with the guavaSoft software 2.1 and BD FACSDiva 8.0.1 respectively. Histograms for cell cycle were generated with FlowJo V10. Statistical analysis of percentage counts was carried out with Graphpad Prism version 5 using the unpaired *t*-test. P-values ≤ 0.05 were considered to be significant.

3. Results

3.1. B. pilosa possesses selective antitrypanosomal potency

Fractions BPFH (*B. pilosa*, hexane fraction), BPFD (*B. pilosa*, dichloromethane fraction), BPFM (*B. pilosa*, methanol fraction) and BPWB (*B. pilosa*, water-butanol fraction) were prepared from the whole plant of *B. pilosa* using a modified approach of the Kupchan method of solvent extraction (Supplementary Fig. S1). The fractions were tested for their antitrypanosomal activities in a 48-h cell viability assay. BPFD and BPFM were the two fractions that displayed promising antitrypanosomal activities with IC_{50} values of 3.29 and 5.86 μg/ml, respectively (Table 1, Fig. S2). Jurkat (acute lymphoblastic leukemia cells) and Chang liver cells (HeLa

Table 1
Effect of Kupchan fractions on cell viability of *T. brucei*, Chang and Jurkat cells.

FRACTIONS	MEAN IC_{50} ± SEM (μg/mL)			SI	
	T. brucei	Jurkat	Chang liver	Jurkat	Chang liver
BPC	6.72 ± 0.04	NA	NA	NA	NA
BPFD	3.29 ± 0.03	9.57 ± 0.10	115.45 ± 0.05	2.91	35.09
BPFH	6.64 ± 0.05	NA	NA	NA	NA
BPFM	5.86 ± 0.04	16.52 ± 0.03	147.10 ± 0.03	2.82	25.10
BPWB	12.97 ± 0.12	NA	NA	NA	NA
DA	0.57 ± 0.15	NA	37.52 ± 0.02	NA	65.83
DX	NA	0.30 ± 0.25	141.52 ± 0.03	NA	NA

Mean IC_{50} values and standard errors of the mean (SEM) were calculated from three distinct experiments. SI was calculated as the ratio of IC_{50} in Jurkat or Chang liver cells to the IC_{50} in *T. brucei*. BP= *B. pilosa* L., whole plant; BPC = crude extract of BP; FD = Dichloromethane fraction; FM = methanol fraction; WB = water-butanol fraction; FH = hexane fraction; DA = Diminazene aceturate, (antitrypanosomal drug); DX = Doxorubicin, (antileukaemia drug); SI = selectivity index; NA=Not applicable (based on activities against *T. brucei*, only BPFD and BPFM were further investigated for their effects on Chang and Jurkat cells); DA and DX were used as positive controls.

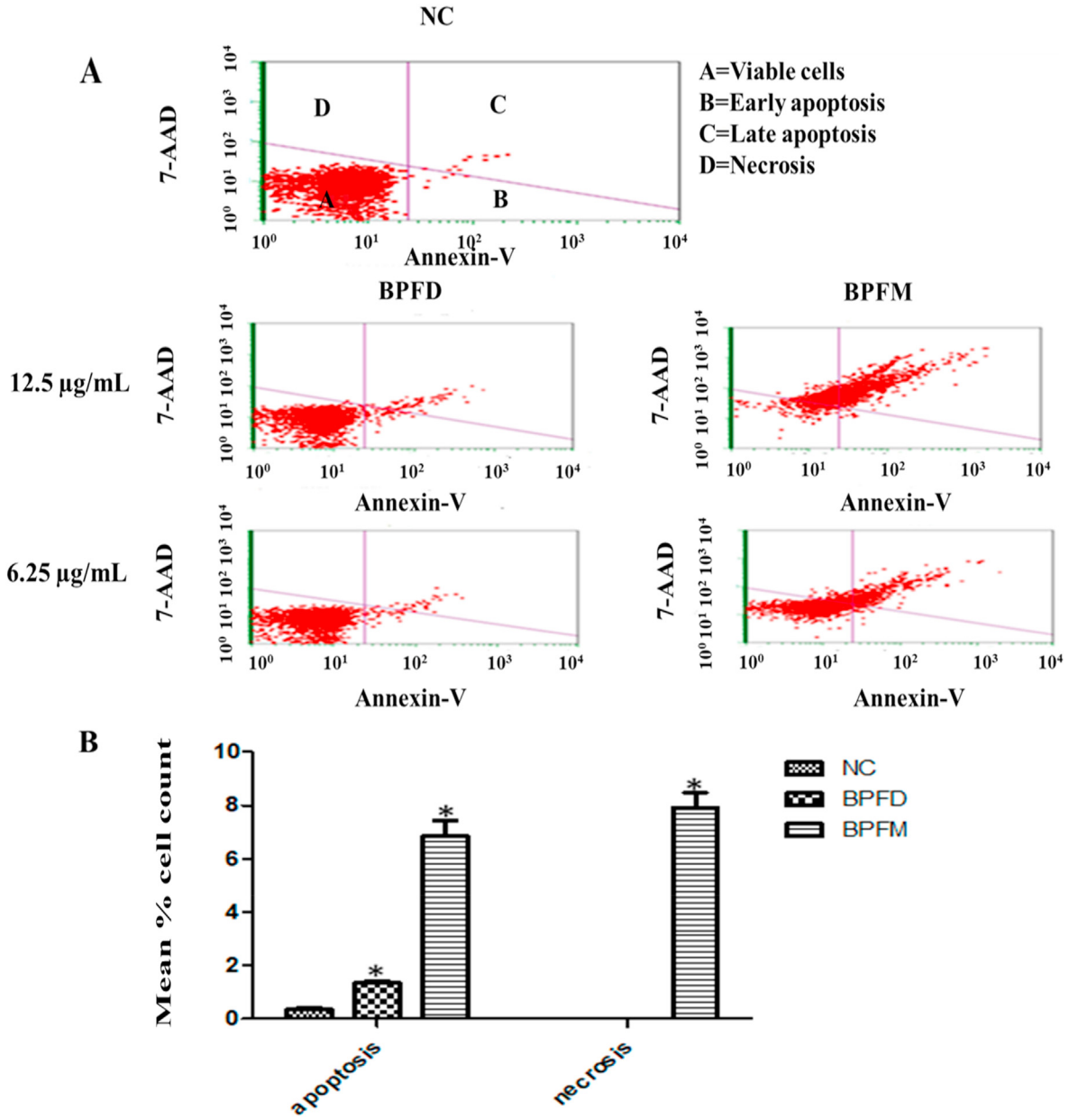

Fig. 1. Effect of fractions BPFD and BPFM on induction of cell death in *T. brucei*.
A. Interaction between phycoerythrin-bound annexin-V protein (X-axis) and phosphatidyl serine released from the cytoplasmic portion of the plasma membrane to the periphery during either early apoptosis or late apoptosis, was investigated. Binding between 7-amino-actinomycin D (7-AAD, Y-axis) and the fragmented DNA during either late apoptosis or necrosis, was also analysed. Experiment was performed at two-fold dilutions of fractions. **B.** P-values were calculated from 3 different counts (n=3) [P <0.05 (*)]. Error bars originate from mean percentage count ± standard deviation of the mean (Mean ± SD). Cells were counted at the IC_{50} values of fractions. BP=*B. pilosa* L., whole plant; FD=Dichloromethane fraction; FM=Methanol fraction; NC=Negative control.

derivatives) were also included to investigate cytotoxicity and selectivity profiles of BPFM and BPFD. Both fractions were more selective to *T. brucei* as compared to Jurkat or Chang liver cells, even though the selectivity for *T. brucei* was higher with Chang liver cells (BPFD, SI = 35.09; BPFM, SI = 25.10) (Table 1). Interestingly, BPFM and BPFD also exhibited promising antileukaemia activities with respective IC_{50} values of 16.52 and 9.57 µg/ml (Table 1). However, both fractions were relatively selective to *T. brucei* as compared to Jurkat cells (BPFD, SI = 2.91; BPFM, SI = 2.82) (Table 1). The fractions also exhibited inverted sigmoidal dose-response curves with Hill coefficients less than −1 (Fig. S2), suggesting a positively cooperative mode of interaction with binding sites of potential receptors or targets.[23]

3.2. *B. pilosa induces apoptosis-like and necrosis-like cell death in T. brucei*

Since BPFM and BPFD were the fractions displaying promising trypanocidal activity, they were chosen for further investigation into the mechanisms of action against *T. brucei*. Insights into the mechanisms of cell death can facilitate drug discovery in AT. Parasites challenged with fractions at varying concentrations for 24 h were used in a cell death analysis. While each fraction caused early and late apoptosis-like cell death in *T. brucei*, induction of necrosis-like cell death was evident in only BPFM-treated cells (Fig. 1A). A two-fold increase in fraction concentration resulted in a dose-dependent increase in apoptosis- and necrosis-like cell death

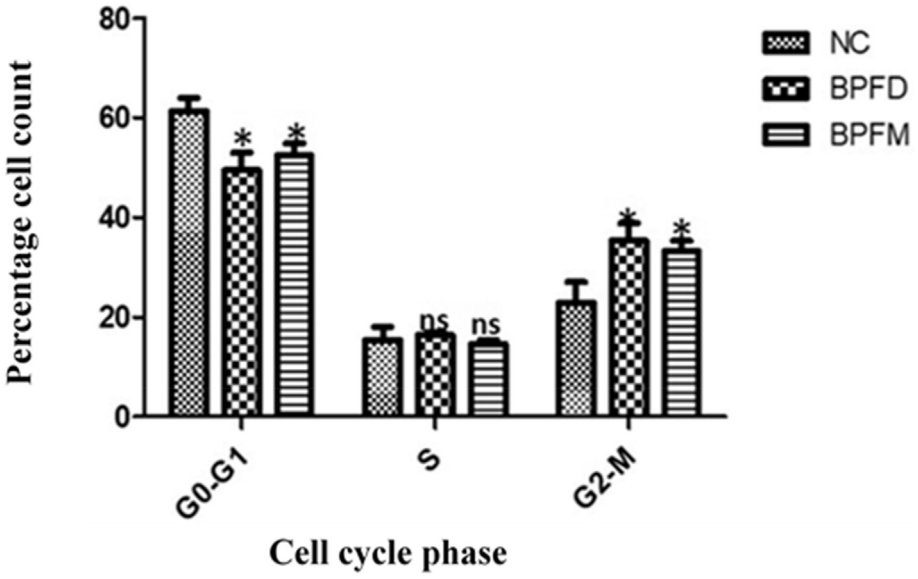

Fig. 2. Effect of fractions BPFD and BPFM on cell cycle of *T. brucei*.
P-values were calculated from 4 distinct counts (n=4): [P <0.05 (*); P≥0.05 (ns)]. Error bars are from mean percentage count ± standard deviation of the mean (Mean ± SD); BP= *B. pilosa* L., whole plant; FD=Dichloromethane fraction; FM=Methanol fraction; NC=Negative control.

(Fig. 1A). This increase was more prominent in BPFM as compared to BPFD (Fig. 1A). At the IC_{50} values, BPFD and BPFM caused an induction of apoptosis-like cell death from approximately 0.36% of cells in the negative control to 1.34% ($p = 0.0003$) and 6.85% ($p = 0.0004$) in treated cells, respectively, while BPFM induced necrosis-like cell death in 7.90% of cells ($p = 0.0002$) (Fig. 1B).

3.3. Effects of B. pilosa on cell cycle phases and morphology of T. brucei

To determine whether the fractions caused any effects on distinct cell cycle phases of *T. brucei*, analysis of cell cycle was performed by employing the interaction between propidium iodide and DNA (Fig. 2, Fig. S3). Parasites were challenged with the fractions at the IC_{50} values. Three distinct phases of the cell cycle in *T. brucei* were identified: G0-G1, S and G2-M phases. There was a significant reduction in the G0-G1 phase cells from 61.18% in the negative control to 49.48% ($p = 0.0014$) and 52.48% ($p = 0.0021$) in BPFD- and BPFM-treated cells respectively (Fig. 2). This represented a reduction of 11.7 and 8.7% points in G0-G1 cells as induced by BPFD and BPFM respectively. There was also a significant increase of G2-M phase cells from 22.89% in the untreated control to 35.38% ($p = 0.0035$) in BPFD and 33.20% ($p = 0.0043$) in BPFM representing an increase of 12.49 and 10.31% points respectively (Fig. 2). However, there was no significant change in S phase cells for both fractions (Fig. 2). BPFM also induced a distinct subpopulation of parasites with a higher DNA content at the G2-M phase (Fig. S3). After treatment for 24 h at the IC_{50} values of the fractions, clumpy and rounded subpopulations of parasites were observed in contrast to the usual slender shape of untreated parasites, especially for cells treated with BPFD (Fig. 3).

3.4. Isolation and characterization of tryptophan alkyl esters from methanol fraction of B. pilosa

As BPFM showed a more pronounced effect on the trypanosomes, this fraction was selected for isolation and characterization of compounds responsible for the trypanocidal activity. Compounds **1** and **2** were eluted at respective retention times of 35.122 and 33.320 min as indicated in the HPLC chromatograms (Fig. S4). In a GC-MS analysis, compounds **1** and **2** were separated at retention times of 27.096 and 24.045 min (Fig. S5), and identified as butyl and propyl esters of tryptophan with *m/z* of 261.16 and 247.14, respectively (Figs. S6 and S7). After identification of the compounds, cell viability analysis was employed to confirm their antitrypanosomal potencies as compared to diminazene aceturate (DA), a known commercially available antitrypanosomal drug. Compounds **1** and **2** exhibited significant antitrypanosomal effects on *T. brucei* with IC_{50} values of 0.66 and 1.46 μg/ml, respectively (Table 2, Fig. S8), suggesting that these compounds contributed significantly towards the growth inhibition of *T. brucei* observed for fraction BPFM. The compounds also displayed relatively non-toxic selectivity profiles with regards to effects on normal macrophages RAW 264.7 cell lines (compound **1**, SI = 95.21; compound **2**, SI = 82.05) (Table 2, Fig. S8). Both compounds were therefore comparable to DA in terms of potency and selectivity profiles (Table 2, Fig. S8).

3.5. Effects of butyl and propyl esters of tryptophan on cell cycle phases and morphology of T. brucei

The mechanisms of action of propyl and butyl esters of tryptophan against the cell cycle of *T. brucei* were also investigated at the IC_{50} values (Fig. 4). There was a significant reduction of G0-G1 phase from 61.40% in the negative control to 38.17% ($p = 0.0025$) and 42.23% ($p = 0.0039$), representing a reduction of 23.23 and 19.17% points in G0-G1 cells as induced by compound **1** and **2**, respectively (Fig. 4). Again, there was a significant increase of S phase from 14.87% in untreated cells to 27.60% ($p = 0.0028$) and 26.20% ($p = 0.0032$), which represented an increase of 12.73 and 11.33% points in S cells as induced by compound **1** and **2** respectively (Fig. 4). Finally, there was a significant increase of G2-M phase from 21.90% in the negative control to 42.47% ($p = 0.0019$) and 39.50% ($p = 0.0021$), which was equivalent to an increase of 20.57 and 17.60% points in G2-M cells in compound **1**- and **2**-treated cells respectively (Fig. 4). Comparatively, DA resulted in a reduction of 28.8% points ($p = 0.0031$), increase of 2.43% points ($p = 0.0041$) and an increase of 12% points ($p = 0.0025$) in G0-G1, S

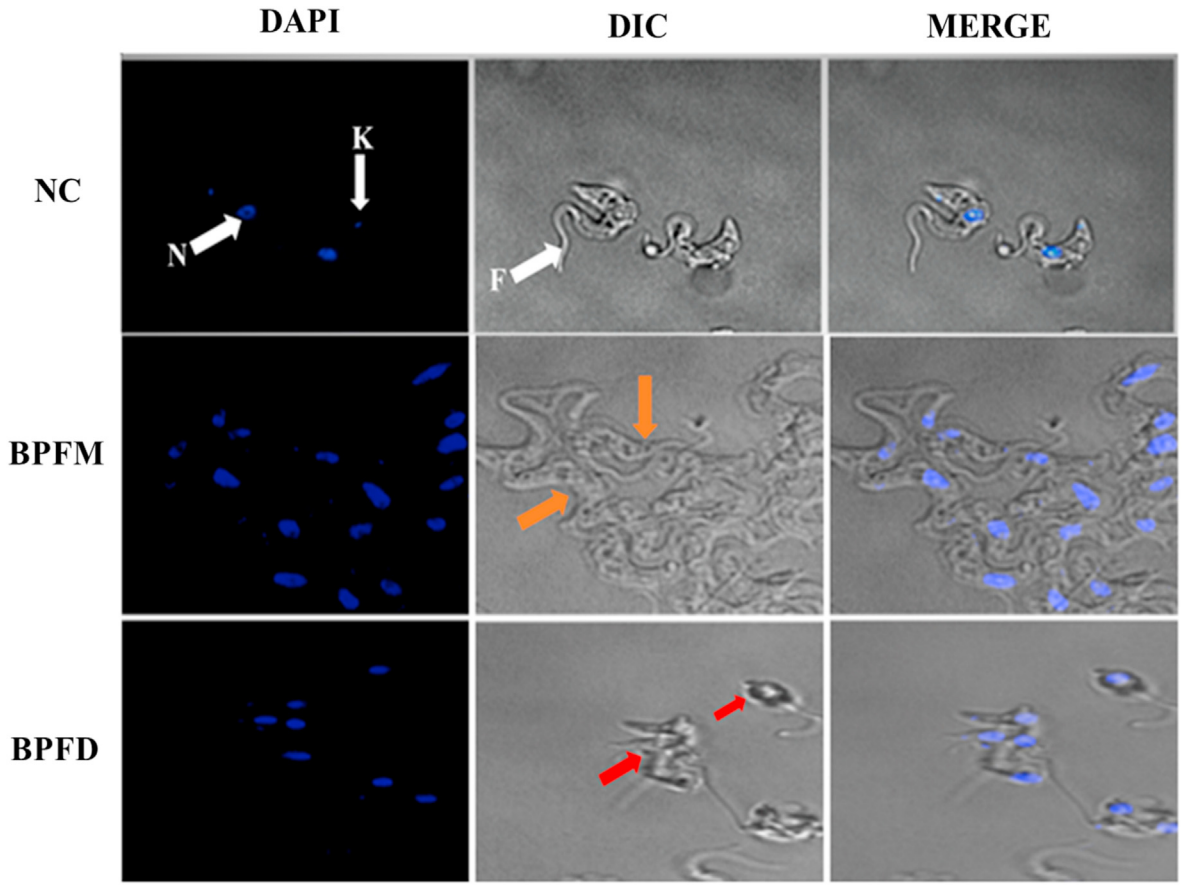

Fig. 3. Effects of BPFD and BPFM on cell morphology and distribution of *T. brucei*.
White arrows (N=nucleus, K=kinetoplast, F=flagellum); Orange arrows=BPFM-treated cells; Red arrows=BPFD-treated cells; BP=*B. pilosa*, whole plant; FD=Dichloromethane fraction; FM=Methanol fraction; NC=Negative control; DIC=Differential interference contrast.

Table 2
Antitrypanosomal activities and chemical structures of compounds **1** and **2**.

COMPOUND	MEAN IC_{50} (μg/mL) ± SEM	SI	STRUCTURE
Diminazene (Reference drug)	0.83 ± 0.09	89.30	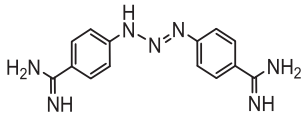
Tryptophan butyl ester (Compound **1**)	0.66 ± 0.01	95.21	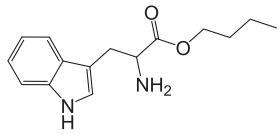
Tryptophan propyl ester (Compound **2**)	1.46 ± 0.09	82.05	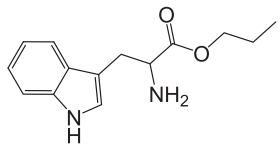

Selectivity index (SI) was calculated as the ratio of IC_{50} in RAW 264.7 cell lines to the IC_{50} in *T. brucei*. SEM = standard error of the mean.

and G2-M phase parasites respectively (Fig. 4). Generally, the graphical pattern of cell cycle alterations for the compounds was similar to that observed for the parent BPFM and BPFD fractions (Fig. S9). However, parasites challenged with compounds for 24 h at the IC_{50} values did not exhibit any significant effects on cell morphology or distribution (Fig. 5).

4. Discussion

The present study set out to investigate potential trypanocidal properties of *B. pilosa* with regards to inhibition of cell cycle, induction of cell death and effects on the morphology of *T. brucei*. The aqueous extract of *B. pilosa* was previously reported to reduce the

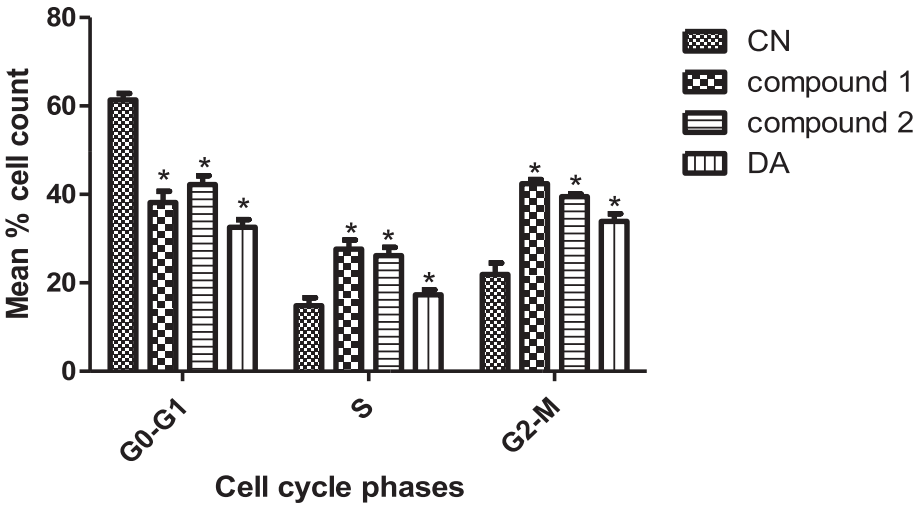

Fig. 4. Effects of compound 1 and 2 on cell cycle of *T. brucei*.
P-values were calculated from 4 distinct counts (n=4): [P <0.05 (*)]. Error bars are from mean percentage count ± standard deviation of the mean (Mean ± SD).

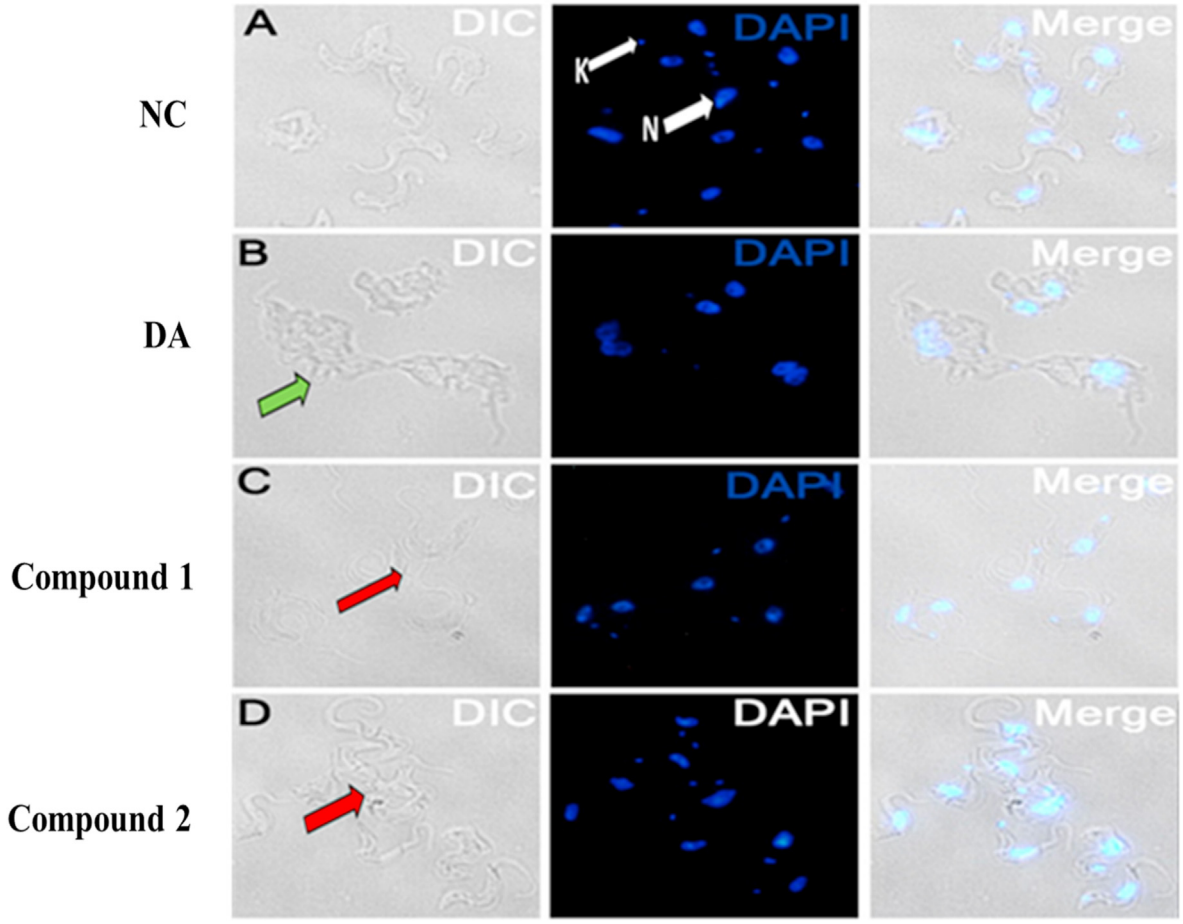

Fig. 5. Effects of compounds on cell morphology and distribution of *T. brucei*.
Green arrow=DA-treated cells, red arrows= compound **1**- and **2**-treated subpopulation of parasites; white arrows (K=kinetoplast, N=nucleus); NC=Negative control; DA= Diminazene aceturate.

expression of proteins involved in the suppression of apoptosis in human T-cell leukemia virus type 1-infected T-cell lines,[24] as well as induce apoptosis in human colon cancer cell lines.[25] However, the present study is the first time B. pilosa is shown to induce apoptosis-like cell death in trypanosomes. The observed inhibitory activity of the plant species on Jurkat cells also corroborates the previously reported effects on human T-cell leukemia virus type 1-infected T-cells.[24]

The aqueous extract of *B. pilosa* was previously reported to induce G1 cell cycle arrest in human T-cell leukemia virus type 1-infected T-cell lines.[24] In this study, we further showed that *B. pilosa* respectively inhibited and arrested the G0-G1 and G2-M phases in trypanosomes. The methanol fraction of *B. pilosa* and its isolated compounds significantly reduced the number of cells in the G0-G1 phase while increasing the G2-M population. Since cytokinesis is tightly connected to the G2-M phase,[26] it is possible that the former was inhibited under the presently investigated conditions. However, further studies into the regulation of karyokinesis and cytokinesis in *B. pilosa*-treated parasites would facilitate the provision of direct and detailed insights.

In contrast to early apoptosis in which degradation of DNA occurs, moderate preservation of DNA may take place during late apoptosis or necrosis. There is nonetheless a loss of integrity of the plasma membrane as well as the disruption of cytoplasmic organelles during late apoptosis or necrosis.[27] This has the possibility of inducing subpopulation of parasites with high DNA content at the expense of corresponding cytokinesis. In this context, the observed clumpy subpopulation of BPFM-treated parasites may depict an inclination towards the induction of late apoptosis or necrosis as compared to early apoptosis. However, further studies involving statistical analysis of clumping rate in control and treated parasites are required to establish any possible link between mechanisms of cell death and potential aggregating effects of *B. pilosa* on *T. brucei*.

The essential role played by tryptophan in the growth of trypanosomes is well established. A rapid *in vitro* uptake of tryptophan and a reduction in serum tryptophan levels probably linked to an increase in indoleamine 2,3-dioxygenase have been reported.[28] This was subsequently corroborated *in vivo* through a significant increase in parasitemia following an inhibition of indoleamine 2,3-dioxygenase.[28] Moreover, the kynurenine pathway of tryptophan metabolism was shown to be activated and associated with inflammation of the central nervous system during the late stage of human African trypanosomiasis in rodent models.[29] Furthermore, the possibility of tryptophan aminoglycoside to interfere with the normal uptake and metabolism of tryptophan in *T. brucei* was previously reported.[30] Collectively, it is expected that a derivative of tryptophan would interfere with tryptophan metabolism to control the growth of *T. brucei*.

Despite the promising antitrypanosomal inhibitory concentrations, the present study suggested disparities in efficacies between individual tryptophan esters and the parent fraction in terms of the overall effects on parasite morphology and distribution. A plausible scenario might be that synergistic interactions between the compounds play a key role as far as attainment of maximum efficacy against *T. brucei* is concerned. It is also possible that as separate compounds, tryptophan esters might possess certain physicochemical limitations that would require pharmacological optimization to attain the needed chemotherapeutic properties, as it is with a number of isolated natural compounds.[31] It might also be the case that other minor secondary metabolites of *B. pilosa* not identified in the present study contributed towards the trypanocidal effects of parent fractions. Overall, further studies into the mechanisms of action of the tryptophan esters are required to provide insights into these possibilities. The outcome of such investigations may also facilitate useful drug discovery approaches in the context of broad existing strategies employed in the discovery of novel chemotherapy for tropical diseases.[32]

In a broader context, the present study highlights the prospects of essential amino acids in the drug discovery and development process for protozoans. Essential amino acids represent key drug discovery targets due to the absence of their metabolic pathways in mammals. This could be the rationale behind the structural mimicking of essential amino acids as evident in some commercially available drugs. Indeed, the human African antitrypanosomal drug eflornithine, which is currently employed as a combination therapy with nifurtimox,[33] mimics the backbone of lysine. Thus, halogenation and esterification provide clues by which drug discovery strategies may take advantage of essential amino acids and their biosynthetic pathways to widen the base of the search for novel anti-protozoan chemotherapies.

Funding statements

This work was supported by funds from a World Bank African Centres of Excellence grant (ACE02-WACCBIP: Awandare) and a DELTAS Africa grant (DEL-15-007: Awandare). The DELTAS Africa Initiative is an independent funding scheme of the African Academy of Sciences (AAS)'s Alliance for Accelerating Excellence in Science in Africa (AESA) and supported by the New Partnership for Africa's Development Planning and Coordinating Agency (NEPAD Agency) with funding from the Wellcome Trust (107755/Z/15/Z: Awandare) and the UK government. The views expressed in this publication are those of the authors and not necessarily those of AAS, NEPAD Agency, Wellcome Trust or the UK government. The work was also partially supported by the Japan Initiative for Global Research Network on Infectious Diseases (J-GRID) from Ministry of Education, Culture, Sport, Science & Technology in Japan, and Japan Agency for Medical Research and Development (AMED).

Declaration of competing interest

Authors declare that there is no conflict of interest.

Acknowledgement

Jurkat, Chang liver (HeLa derivative) and RAW 264.7 cell lines were generously provided by Professor (Mrs.) Regina Appiah-Opong, Department of Clinical Pathology, Noguchi Memorial Institute for Medical Research, University of Ghana. We are grateful to Herone Blagogee of the Center for Plant Medicine Research (CPMR), Mampong-Akuapem, Ghana, for the identification and authentication of *B. pilosa*.

Appendix A. Supplementary data

Supplementary data to this article can be found online at https://doi.org/10.1016/j.jtcme.2021.08.008.

References

1. Simarro PP, Cecchi G, Franco JR, et al. Estimating and mapping the population at risk of sleeping sickness. *PLoS Neglected Trop Dis*. 2012;6:e1859.
2. Morrison LJ, Vezza L, Rowan T, Hope JC. Animal african trypanosomiasis: time to increase focus on clinically relevant parasite and host species. *Trends Parasitol*. 2016;32:599–607.
3. Cnops J, Magez S, De Trez C. Escape mechanisms of African trypanosomes: why trypanosomosis is keeping us awake. *Parasitology*. 2015;142:417–427.
4. Melaku A, Birasa B. Drugs and drug resistance in african animal trypanosomosis: a review. *Eur J Appl Sci*. 2013;5:84–91.
5. Steverding D. The development of drugs for treatment of sleeping sickness: a historical review. *Parasites Vectors*. 2010;3:15.
6. Barrett MP, Vincent IM, Burchmore RJ, Kazibwe AJ, Matovu E. Drug resistance in human African trypanosomiasis. *Future Microbiol*. 2011;6:1037–1047.
7. Franco JR, Simarro PP, Diarra A, Ruiz-Postigo JA, Samo M, Jannin JG. Monitoring the use of nifurtimox-eflornithine combination therapy (NECT) in the treatment of second stage gambiense human African trypanosomiasis. *Res Rep Trop Med*. 2012;3:93–101.
8. Matovu E, Geiser F, Schneider V, et al. Genetic variants of the TbAT1 adenosine transporter from African trypanosomes in relapse infections following melarsoprol therapy. *Mol Biochem Parasitol*. 2001;117:73–81.
9. Scott AG, Tait A, Turner CM. Characterisation of cloned lines of Trypanosoma brucei expressing stable resistance to MelCy and suramin. *Acta Trop*. 1996;60:

251–262.
10. Tagboto S, Townson S. Antiparasitic properties of medicinal plants and other naturally occurring products. *Adv Parasitol*. 2001;50:199–295.
11. Pozharitskaya ON, Shikov AN, Makarova MN, et al. Anti-inflammatory activity of a HPLC-fingerprinted aqueous infusion of aerial part of Bidens tripartita L. *Phytomedicine*. 2010;17:463–468.
12. Bartolome AP, Villasenor IM, Yang WC. Bidens pilosa L. (Asteraceae): botanical properties, traditional uses, phytochemistry, and pharmacology. *Evid Based Complement Alternat Med*. 2013;2013:340215.
13. Ge C. Cytologic study of Bidens bipinnata L. *Zhongguo Zhongyao Zazhi*. 1990;15:72–74, 125.
14. Young PH, Hsu YJ, Yang WC. Bidens pilosa L. and its medicinal use. In: Awaad AS, Singh VK, Govil JN, eds. *Recent Progress in Medicinal Plants Drug Plant II*. Houston, Texas, USA: Standium Press; 2010.
15. Silva FL, Fischer DC, Tavares JF, Silva MS, de Athayde-Filho PF, Barbosa-Filho JM. Compilation of secondary metabolites from Bidens pilosa L. *Molecules*. 2011;16:1070–1102.
16. Mwaniki LM, Mose JM, Mutwiri T, Mbithi JM. Evaluation of trypanocidal activity of bidens pilosa and physalis peruviana against trypanosoma brucei rhodesiense. *Am J Lab Med*. 2017;2:69–73.
17. Peter O, Magiri E, Auma J, Magoma G, Imbuga M, Murilla G. Evaluation of in vivo antitrypanosomal activity of selected medicinal plant extracts. *J Med Plants Res*. 2009;3:849–854.
18. Kupchan SM, Britton RW, Ziegler MF, Sigel CW. Bruceantin, a new potent antileukemic simaroubolide from Brucea antidysenterica. *J Org Chem*. 1973;38:178–179.
19. Vega-Avila E, Pugsley MK. An overview of colorimetric assay methods used to assess survival or proliferation of mammalian cells. *Proc West Pharmacol Soc*. 2011;54:10–14.
20. Wlodkowic D, Skommer J, Darzynkiewicz Z. Flow cytometry-based apoptosis detection. *Methods Mol Biol*. 2009;559:19–32.
21. Dofuor AK, Djameh GI, Ayertey F, et al. Antitrypanosomal effects of *Zanthoxylum zanthoxyloides* (lam.) zepern. & timler extracts on african trypanosomes. *Evid Based Complement Alternat Med*. 2019;2019:1730452.
22. Pozarowski P, Darzynkiewicz Z. Analysis of cell cycle by flow cytometry. *Methods Mol Biol*. 2004;281:301–311.
23. Prinz H. Hill coefficients, dose-response curves and allosteric mechanisms. *J Chem Biol*. 2010;3:37–44.
24. Nakama S, Ishikawa C, Nakachi S, Mori N. Anti-adult T-cell leukemia effects of Bidens pilosa. *Int J Oncol*. 2011;38:1163–1173.
25. Takamatsu R, Tokeshi AM, Nakama K, Yoshimi N. P0159 Bidens pilosa extract induces apoptosis through up-regulation of death receptor 5 in human colon carcinoma cell lines. *Eur J Canc*. 2014;50:e54.
26. Vaughan S, Gull K. The structural mechanics of cell division in Trypanosoma brucei. *Biochem Soc Trans*. 2008;36:421–424.
27. Szallies A, Kubata BK, Duszenko M. A metacaspase of *Trypanosoma brucei* causes loss of respiration competence and clonal death in the yeast *Saccharomyces cerevisiae*. *FEBS Lett*. 2002;517:144–150.
28. Vincendeau P, Lesthelle S, Bertazzo A, Okomo-Assoumou MC, Allegri G, Costa CVL. Importance of L-tryptophan metabolism in trypanomiasis. In: *Tryptophan, Serotonin and Melatonin; Basic Aspects and Applications. Huether et al.* New York: Kluwer Academic/Plenum Publishers; 1999:525–535.
29. Sternberg JM, Forrest CM, Dalton RN, et al. Kynurenine pathway activation in human african trypanosomiasis. *J Infect Dis*. 2017;215:806–812.
30. Kyeremeh K, Kwain S, Tetevi GM, et al. α-d glucopyranosyl-(1→2)-[6-O-(L-tryptophanyl)-d-fructofuranoside]. *Molbank*. 2019, eM1066.
31. Chen J, Li W, Yao H, Xu J. Insights into drug discovery from natural products through structural modification. *Fitoterapia*. 2015;103:231–241.
32. Nwaka S, Hudson A. Innovative lead discovery strategies for tropical diseases. *Nat Rev Drug Discov*. 2006;5:941–955.
33. Priotto G, Kasparian S, Mutombo W, et al. Nifurtimox-eflornithine combination therapy for second-stage African Trypanosoma brucei gambiense trypanosomiasis: a multicentre, randomised, phase III, non-inferiority trial. *Lancet*. 2009;374(9683):56–64.